Since January 2020 Elsevier has created a COVID-19 resource centre with free information in English and Mandarin on the novel coronavirus COVID-19. The COVID-19 resource centre is hosted on Elsevier Connect, the company's public news and information website.

Virus Research 194 (2014) 90–99

Contents lists available at ScienceDirect

Virus Research

journal homepage: www.elsevier.com/locate/virusres

Insights into RNA synthesis, capping, and proofreading mechanisms of SARS-coronavirus

Marion Sevajol [1], Lorenzo Subissi [1], Etienne Decroly, Bruno Canard, Isabelle Imbert *

Centre National de la Recherche Scientifique, Aix-Marseille Université, UMR 7257, AFMB, 163 Avenue de Luminy, 13288 Marseille, France

ARTICLE INFO

Article history:
Available online 17 October 2014

Keywords:
SARS coronavirus
Replication
Capping
Proofreading

ABSTRACT

The successive emergence of highly pathogenic coronaviruses (CoVs) such as the Severe Acute Respiratory Syndrome (SARS-CoV) in 2003 and the Middle East Respiratory Syndrome Coronavirus (MERS-CoV) in 2012 has stimulated a number of studies on the molecular biology. This research has provided significant new insight into functions and activities of the replication/transcription multi-protein complex. The latter directs both continuous and discontinuous RNA synthesis to replicate and transcribe the large coronavirus genome made of a single-stranded, positive-sense RNA of ~30 kb.

In this review, we summarize our current understanding of SARS-CoV enzymes involved in RNA biochemistry, such as the *in vitro* characterization of a highly active and processive RNA polymerase complex which can associate with methyltransferase and 3′–5′ exoribonuclease activities involved in RNA capping, and RNA proofreading, respectively. The recent discoveries reveal fascinating RNA-synthesizing machinery, highlighting the unique position of coronaviruses in the RNA virus world.

1. Introduction

The evolution rates of RNA viruses are amongst the highest of all organisms, making phylogenetic comparison between viral families often challenging. The *Nidovirales* order consists of four families that display broadly diverse features: from genome length spanning from 13 to 32 kb, to the set of encoded genes, or host range. Nonetheless, all nidoviruses share common characteristics such as the use of ribosomal frameshifting in order to translate a part of the nonstructural proteins, including the RNA-dependent RNA polymerase and the helicase. Moreover, they all code for a set of subgenomic (sg) mRNAs, and also for six essential enzyme/protein domains displaying the same linear organization along the genome: a 3C-like proteinase (3CLpro) flanked by 2 transmembrane domains (TM), then the RNA-dependent RNA polymerase (RdRp) and eventually a zinc-cluster binding domain (Zm) fused to a helicase belonging to superfamily 1 (HEL1). This specific protein organization can be summarized as follows: Nter-TM2-3CLpro-TM3-RdRp-(Zm)-HEL1-Cter.

The *Coronaviridae* together with the *Roniviridae* and the *Mesoniviridae* families are called "large-genome nidoviruses", because their genome length spans from 20 kb to 32 kb. In contrast, viruses of the fourth family, the *Arteriviridae*, belongs to the so-called "small-genome nidoviruses", since their genome length is between 13 and 16 kb (Gorbalenya et al., 2006).

Among *Nidovirales*, only some coronaviruses (CoVs) are known to infect humans. Human coronaviruses mostly cause mild respiratory infections. However, in 2003, a new coronavirus was identified to be responsible of a Severe Acute Respiratory Syndrome (SARS) (Stadler et al., 2003). SARS-CoV eventually spread across the globe, causing a total of around 8400 infections and with a case/fatality rate (CFR) of 10%. Studies following the pandemic showed that SARS-CoV is a zoonotic virus jumping from bats to humans upon undefined critical mutational events, and possibly through palm civets as intermediate hosts (Li et al., 2005; Wang and Eaton, 2007). Recently, the direct progenitor virus of SARS-CoV from bat has been isolated (Ge et al., 2013). This bat SARS-like CoV uses the human angiotensin converting enzyme II (ACE2) receptor and live viruses were recovered from Vero E6 cells (Ge et al., 2013). Hence, this virus does not require any mutations or intermediate hosts to infect human cells.

A decade after the SARS crisis, a new coronavirus was identified in the Middle East causing a form of pneumonia associated in some instances to kidney failure (De Groot et al., 2013; Zaki et al., 2012). This coronavirus is now named Middle East Respiratory Syndrome Coronavirus (MERS-CoV), and the epidemic is still ongoing

* Corresponding author at: Architecture et Fonction des Macromolécules Biologiques, CNRS and Aix-Marseille Université, UMR 7257, ESIL/Polytech Case 925, 13288 Marseille, France. Tel.: +33 491 82 86 28; fax: +33 491 82 86 46.
E-mail address: isabelle.imbert@afmb.univ-mrs.fr (I. Imbert).
[1] These authors contributed equally to this work.

http://dx.doi.org/10.1016/j.virusres.2014.10.008
0168-1702/

two years after its discovery, counting at present (July 2014) 837 cases with the CFR of approximately 30%. MERS-CoV seems to be also of a zoonotic origin, as antibodies against MERS-CoV have been detected in camels (Perera et al., 2013; Reusken et al., 2013) and a case of camel-to-human transmission has been recently reported (Azhar et al., 2014).

These two episodes confirm that few mutations allow zoonotic coronaviruses to jump the species barriers and threat human health worldwide. To date, no specific treatment against CoVs is available. A better understanding about how coronaviruses replicate in the host is therefore of critical importance to develop antiviral strategies aiming at controlling their spread and morbidity.

Coronavirus RNA replication and transcription are mediated by nonstructural proteins (nsps) encoded by two open reading frames, ORF1a and ORF1b (Fig. 1). These two ORFs are translated in a cap-dependent manner to yield two overlapping polyproteins referred as pp1a and pp1ab. ORF1b is translated only upon a ribosomal frameshift (−1) near the 3′ end of ORF1a, with ∼30% efficacy (Snijder et al., 2003). Hence, the nsps encoded in ORF1b (nsp12 to nsp16) are expressed at lower levels compared to ORF1a-encoded products (nsp1 to nsp11). After polyprotein maturation mediated by viral proteases, these nsps associate to form a large replicative/transcription complex (RTC) with yet unknown cellular factors. The RTC not only entails the synthesis of new viral genomes from a full-length negative-stranded template, but also a nested set of so-called subgenomic (sg) mRNAs encoding structural and accessory proteins (Fig. 1) (Pasternak et al., 2006). Coronavirus genome encodes for a total of 16 nsps, many having predicted and/or experimentally established function, and some others with yet defined functions.

Among them, the RNA-dependent RNA polymerase (RdRp) encoded by nsp12 plays a central role in both RNA replication and transcription of the viral RNA. In general, RNA virus RdRps deal with genomes spanning from 5 to 15 kb in length. Coronavirus RdRps stand out as they not only replicate large RNA molecules (up to 32 kb) but also transcribe the nested set of sg mRNAs. Coronaviruses also possess other activities typically found in (+) RNA viruses, such as helicase and capping enzymes. On the other hand, less common or even unique RNA-processing activities are associated with other nsps, such as two nuclease activities: a 3′–5′ Exonuclease (ExoN) in the amino-terminal domain of nsp14 (Minskaia et al., 2006), and an endoribonuclease (NendoU) in nsp15 (Ivanov et al., 2004a). While the role of the former begins to be well established in proofreading, the role of the latter is still unclear.

Coronaviruses also encode for another group of unique and interesting proteins: nsp7 to nsp10, which are all small proteins with no known protein homolog. Initially, they were all described as RNA binding proteins (Egloff et al., 2004; Su et al., 2006; Zhai et al., 2005). In more recent works, three of them (nsp7, nsp8 and nsp10) were shown to act as activating co-factors of the polymerase (nsp7, nsp8), the 3′–5′ ExoN (nsp10) and the 2′O-methyltransferase (MTase) (nsp10) activities.

In this review, we present the current state of knowledge on SARS-CoV enzymes involved in RNA synthesis, proofreading, and capping.

2. Formation of the replicative/transcription complex (RTC)

In coronaviruses, replication refers to viral genome amplification, while transcription refers to the synthesis of nested set of sg mRNAs. Both processes are mediated by the RTC, which is located in a membranous network, called reticulo-vesicular network, which arises from the rearrangements of endoplasmic reticulum (ER) membranes (Knoops et al., 2008). Nsp3, through its transmembrane domain and together with two transmembrane proteins (nsp4 and nsp6) contribute to the anchoring of the RTC to membranes. It may be formed after viral replication cycles in order to hide replication intermediates (dsRNA) from innate immunity sensors (Knoops et al., 2008).

3. The replication/transcription complex catalytic core

As for all (+) RNA viruses, the replication catalytic core contains at least a helicase and an RNA-dependent RNA polymerase (RdRp).

3.1. The NTPase/helicase nsp13

A helicase domain of superfamily 1 helicases is harbored in SARS-CoV nsp13 C-terminal half (Ivanov et al., 2004b). SARS-CoV nsp13 is able to unwind dsRNA (and dsDNA) in a 5′–3′ direction and required energy obtained from the hydrolysis of any NTPs and dNTPs (Ivanov et al., 2004b; Lee et al., 2010; Tanner et al., 2003). The N-terminal region of nsp13 contains a zinc-binding domain forms of 12 conserved cysteine and histidine residues. This domain is conserved in all nidoviruses and is critical for the human CoV-229E (HCoV-229E) helicase activity *in vitro* (Seybert et al., 2005). In order to promote dsRNA unwinding, an RNA substrate of at least five nucleotides in length is required and an estimated unwinding rate of ∼280 base-pairs per second has been calculated, which is similar to other helicases (Adedeji et al., 2012). Interestingly, nsp13-mediated helicase activity has been reported to be stimulated 2-fold by nsp12 RdRp through direct protein/protein interaction (Adedeji et al., 2012).

3.2. Nsp12 RdRp and its cofactors nsp7 and nsp8: a processive polymerase complex

Nsp12 is an RNA-dependent RNA polymerase (RdRp) containing all conserved motifs (named with letters from A to F) of canonical RdRps (Poch et al., 1989). The polymerase active site (Ser-Asp-Asp within motif C) is conserved in all nidoviruses. Nsp12 also carries the motif G (Gorbalenya et al., 2002), which is a signature sequence of RdRps that initiate RNA synthesis in a primer-dependent manner (Te Velthuis et al., 2010). The *in vitro* nsp12 polymerase activity appeared weak and non processive (Cheng et al., 2005; Te Velthuis et al., 2010), at odds with the efficient replication of the very large RNA genome *in vivo*. Protein/protein interaction maps were established for SARS-CoV and among others, the nsp12/nsp8 interaction was recovered (Imbert et al., 2008). The interaction between SARS-CoV nsp7 and nsp8 is also ascertained as they were co-crystallized and proposed to act as processivity factor for nsp12 (Zhai et al., 2005).

In our lab, we tested this hypothesis and detected activation of the primer-dependent polymerase activity of nsp12 upon addition of nsp7 and nsp8 (Subissi et al., 2014b). This nsp7/nsp8/nsp12 complex is also able to synthesize RNA *de novo* in a processive fashion at least up to 340 nucleotides. To better understand how nsp7 and nsp8 activate and confer processivity to the RNA-synthesizing activity of nsp12, we used biochemical assays and a reverse genetics approach. We identified three amino acids in SARS-CoV nsp7 (K7, H36, and N37) that confer RNA-binding properties to the polymerase complex and that are also important for virus replication *in vivo*. Our study also pointed out three nsp8 residues (K58, P183, and R190) critical for SARS-CoV genome replication. The first one is involved in the interaction of the polymerase complex with RNA, while the two others are essential for nsp8/nsp12 interaction.

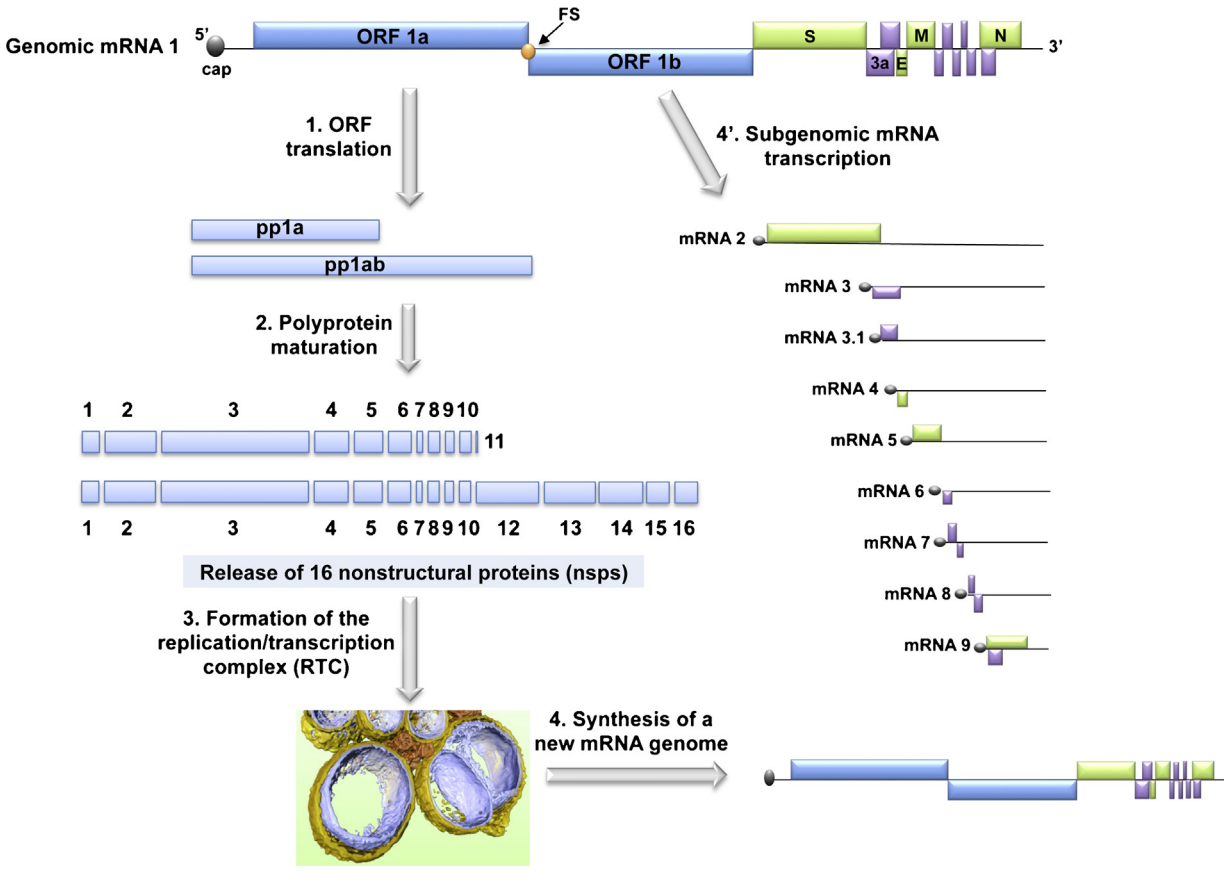

Fig. 1. Coronavirus genome replication and transcription. The two open reading frames (ORFs) of the genomic mRNA are translated by a cap-dependent mechanism, yielding two polyproteins, pp1a and pp1ab, the latter requiring −1 ribosomal frameshifting (FS) near the 3′ end of ORF1a. Subsequently, the two polyproteins are cleaved by two or three ORF1a-encoded proteases to release a total of 16 nonstructural proteins (nsp1–nsp16). Then, they assemble with modified intracellular membranes (Knoops et al., 2008) to form the replication/transcription complex (RTC). This huge RTC not only entails the synthesis of new genomes, but also produces a nested set of subgenomic (sg) mRNAs encoding structural and accessory proteins. The gray ball represents the cap structure. Nonstructural, structural and accessory genes are represented in blue, green and purple, respectively.

3.3. Nsp7 and nsp8, priming and/or processivity factors for nsp12?

Nsp8 of SARS-CoV, feline CoV (FCoV) and HCoV-229E were previously shown to exhibit RNA polymerase activities (Imbert et al., 2006; Te Velthuis et al., 2010; Xiao et al., 2012). Moreover, the nsp8 N-terminal amino-acid composition appears to be important for this activity. Indeed, SARS-CoV nsp8 with an N-terminal His tag can synthesize only short oligonucleotides (<6 nt) (Imbert et al., 2008), while SARS-CoV and FCoV nsp8 without this tag are able to synthesize much longer RNA (Te Velthuis et al., 2010; Xiao et al., 2012). Upon addition of nsp7 to these "improved" recombinant nsp8, the RNA polymerase activity is stimulated (Te Velthuis et al., 2010; Xiao et al., 2012). Notably, the processing intermediates nsp7-nsp10 of HCoV-229E is also able to synthesize oligoribonucleotides (Xiao et al., 2012).

Since nsp12 likely synthesizes RNA in a primer-dependent manner (Gorbalenya et al., 2002), nsp8 was proposed to act as a primase for nsp12. Moreover, SARS-CoV nsp8 crystal structure has been solved in complex with nsp7, showing a hexadecameric structure formed by eight molecules of nsp7 associated with eight nsp8 molecules (Zhai et al., 2005). This structure is reminiscent of processivity factors such as the eukaryotic PCNA sliding clamp (Prelich et al., 1987), and is able to accommodate a dsRNA in its central channel (Fig. 2A) (Zhai et al., 2005).

However, when the nsp8 primase was assayed in the context of the highly active polymerase complex (nsp7/nsp8/nsp12), no short RNAs could be detected (Subissi et al., 2014b). A hypothesis of this discrepancy could be that nsp8 in complex with nsp7 and nsp12 adopted a structural conformation that prevented the synthesis of short RNAs. In other words, nsp7/nsp8 may synthesize primers before associating with nsp12, or nsp7/nsp8-mediated primer synthesis may trigger the formation of the nsp7/nsp8/nsp12 polymerase complex. This possibility is to be examined in light of the tridimensional structure solved for nsp7 and nsp8 from FCoV (Xiao et al., 2012). In this structure, FCoV nsp7 and nsp8 assemble into a heterotrimer formed by one nsp8 molecule associated to two nsp7 molecules, without any central channel (Fig. 2B). SARS-CoV and FCoV nsp8 monomer folds are the same, except the conformation of the N-terminal helical domain that differs due to rotation over one or perhaps two hinge regions in the long alpha-helix, which undergoes partial unfolding at these hinge regions (Fig. 2C) (Xiao et al., 2012; Zhai et al., 2005).

Coronavirus nsp8 in association with nsp7 reveals a remarkable plasticity that may explain several functions triggered by the nature of their partnership and/or quaternary structure.

3.4. The puzzling nsp9 RNA-binding protein

Nsp9 is a small (13 kDa in SARS-CoV) protein unique to coronavirus (Snijder et al., 2003). The two available crystal structures of the protein (Egloff et al., 2004; Sutton et al., 2004) reveal a novel fold made of an open six-stranded β-barrel and an additional α-helix that contains a GXXXG protein/protein interaction motif (Miknis et al., 2009) involved in dimer formation. Noteworthy, this dimerization is critical for virus replication (Miknis et al., 2009).

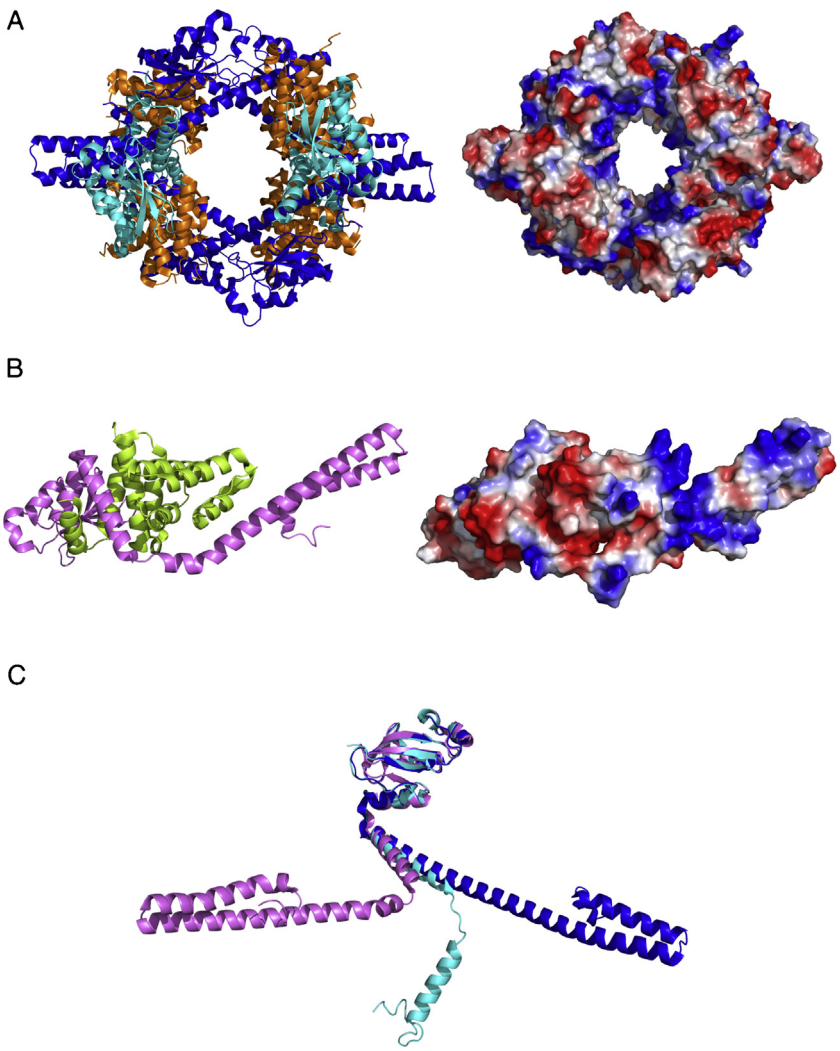

Fig. 2. Coronavirus nsp7/nsp8 structures. (A) Structure of the SARS-CoV nsp7/nsp8 hexadecamer supercomplex (from Zhai et al., 2005; PDB 2AHM). To the left of this panel, SARS-CoV nsp7 and the two conformations of nsp8 are colored in orange, cyan and dark blue, respectively. To the right of this panel, the surface is colored according to electrostatic potential (blue, positive charge; red, negative charge). (B) Structure of the FCoV nsp7/nsp8 heterotrimer (left panel): two nsp7 molecules (in green) are associated to one molecule of nsp8 (in pink) (from Xiao et al., 2012; PDB 3UBO). The right panel shows the surface colored according to electrostatic potential (blue, positive charge; red, negative charge). (C) C-terminal domain superimposition of the two SARS-CoV nsp8 forms (in cyan and dark blue) with FCoV nsp8 (in pink). The amino-terminal domain of nsp8 is very flexible, even in association with nsp7. Images were generated using PYMOL.

In addition, SARS-CoV nsp9 binds ssRNA without sequence specificity (Egloff et al., 2004), and has been shown to interact with nsp8 (Sutton et al., 2004). The DNA replication catalytic core is formed, at least, by the association of a polymerase and its processivity factor, a helicase, and a single-strand DNA-binding protein (SSB). In the case of SARS-CoV, the first three actors were identified in nsp12, nsp8/nsp7 and nsp13, respectively. Regarding the nsp9 structural features, we can hypothesis that this protein may act as an SSB-like molecule thus protecting the CoV RNA genome from degradation during replication.

4. Is the 3′–5′ exonuclease nsp14 an RNA proofreading enzyme?

The study of the coronavirus RNA repair machinery began with the discovery, by A.E. Gorbalenya and co-workers of nuclease motifs in ORF1b of the coronavirus genome. The discovery was published as part of the full analysis of the SARS-CoV genome (Snijder et al., 2003). Amongst other RNA processing enzymes, the authors reported that nsp14 N-terminal domain is an RNA 3′–5′ exonuclease (ExoN) from the DEDD superfamily (Zuo and Deutscher, 2001). They proposed the ExoN activity to be related to RNA proofreading, repair, and/or recombination. These hypotheses were based on DNA organisms, which have developed mechanisms for their large DNA genome biosynthesis and maintenance.

Ubiquitously spread in large-genome viruses, genes encoding homologs of coronavirus nsp14 ExoN are found in all nidoviruses (toro and roniviruses, with respectively 28 and 26 kb genomes), and mesoniviruses (a recently discovered related viral family with a 20 kb genome) (Zirkel et al., 2011). Small genome nidoviruses (arteriviruses, 13–15 kb) do not possess such ExoN activity (reviewed in, Gorbalenya et al., 2006). Outside nidoviruses, nsp14 ExoN homologs are rare, and have been solely identified in arenaviruses so far. In this last case, the ExoN activity is likely involved in counteracting the antiviral innate immunity (Hastie et al., 2011).

The seminal discovery of the CoV 3′–5′ ExoN activity was followed by sequential findings confirming its validity and raised great interest in various fields such as evolution, drug design and drug resistance. The 3′–5′ ExoN enzyme activity was subsequently demonstrated at the enzyme level (Minskaia et al., 2006). The following most compelling demonstration was achieved by Eckerle

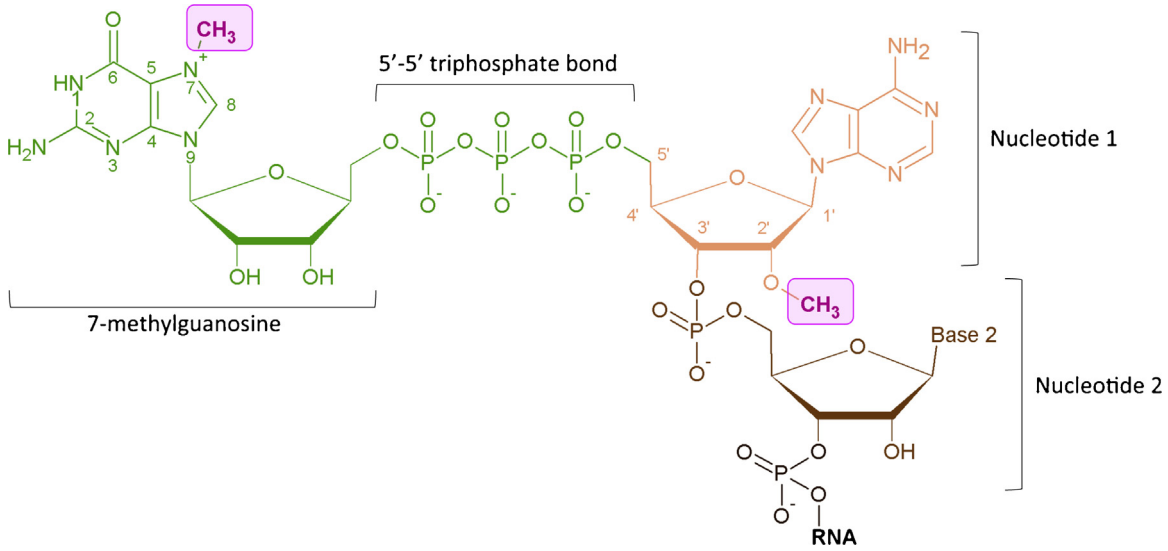

Fig. 3. Structure of 5′-end RNA cap. Cap structure is formed of a N7-methylated guanosine linked to the first RNA nucleotide *via* a 5′–5′ triphosphate bond. A second methyl group is added in 2′O position of the first nucleotide (for SARS-CoV, the first nucleotide is an adenosine).

et al. (2007). These authors showed that mutations in the DEDD motif, usually leading to the inactivation of the exonuclease activity, allowed recovering viable viruses that exhibit a 15–20-fold increase in replication errors. The study was conducted in MHV, a betacoronavirus-like SARS-CoV. Several significant complements and refinements of these studies appeared subsequently (Eckerle et al., 2010). Whereas less than one mutation per sequenced genome was observed for wild-type SARS-CoV (corresponding to an error frequency of 2×10^{-5}), the SARS-CoV ExoN(−) showed 10 mutations per sequenced genome (error frequency = 3×10^{-4}) (Eckerle et al., 2010). The same group recently showed that coronaviruses lacking exoribonuclease activity are susceptible to lethal mutagenesis (Smith et al., 2013). Indeed, they demonstrated that 5-fluorouracil (5FU) is incorporated into SARS-CoV and MHV RNA genomes, driving increased mutagenesis in ExoN(−) viruses (Smith et al., 2013). In addition, ribavirin, a guanosine analog, was also tested on a MHV ExoN(−) strain exhibiting up to 300-fold increased in sensitivity to this compound.

At the enzyme level, mechanistic studies showed that nsp14 ExoN activity is strongly enhanced (>35-fold) by the addition of nsp10 (Bouvet et al., 2012). The nsp10/nsp14 ExoN complex was shown to be dsRNA-specific, but also able to excise one 3′ mismatched nucleotide mimicking a polymerase-mediated nucleotide misincorporation product (Bouvet et al., 2012). It is however unclear which enzyme state, nsp10/14 complex or nsp14 alone is involved in the aforementioned effects on RNA replication errors.

Evidences accumulate in favor of an RNA proofreading system *versus* a post-replicative mismatch repair. The latter generally involves a strand recognition system (*e.g.*, neosynthesized ssRNA methylation) to determine which nucleotide has to be corrected in a mismatch-bearing dsRNA. Then, a succession of enzymatic activities are required to replace the mismatched nucleotide: dsRNA endonucleolytic cleavage, RNA re-synthesis, and RNA ligation. Although several of these activities are embedded in the coronavirus ORF1ab, both strand recognition and ligase activities remain to be determined. In contrast, RNA proofreading generally involves a minimal set of activities of the polymerase dealing with the mismatched nucleotide and, a single 3′–5′ exonuclease activity vicinal to the active RNA polymerase.

To formally demonstrate the occurrence of RNA proofreading by nsp14, several questions have to be addressed, some of which have already been answered. First, nsp14 has to be made available to nsp12, and both should exhibit activities. This has been demonstrated in Subissi et al. (2014b), with the association of nsp12 and nsp14 into an active complex. Second, the RNA mismatch clearance pathway should be reconstituted *in vitro*. That is, not only mismatch formation by nsp12 should be documented (nature and frequency), but also mismatch extension *vs* mismatch excision, yielding an estimate of the mismatch fixation into the RNA genome.

5. Coronavirus cap formation pathway

Eukaryotic messenger RNA translation can be initiated by 2 different signals at the 5′-end, either by a cap structure or by a highly specific RNA tertiary structure named internal ribosome entry site (IRES).

Nidovirus genomes possess a cap structure at their 5′-end (Lai and Stohlman, 1981; Van Vliet et al., 2002). The cap is composed of a methylated guanosine at position N7 and linked to the first transcribed nucleotide of the RNA by a 5′–5′ triphosphate bridge, called "cap-0" (^{7m}GpppN) (Fig. 3). A "cap-0" structure can then be converted into "cap-1" (^{7m}Gppp$_{m2}$N) by the addition of a methyl group to the 2′ position of the first RNA nucleotide (Furuichi and Shatkin, 2000) (Fig. 3). The cap structure is then recognized by the eukaryotic initiation factor 4E (eIF4E), which, in association with other eIFs, recruit the small ribosomal subunit 40S (for review, Decroly et al., 2012). Another cap function was described as protecting the mRNA from cellular 5′-3′ ExoN degradation (Furuichi et al., 1977). Recently, it has been shown that the 2′-O-methylation of the viral cap prevents viral genome recognition by the innate immune system of the host cell (Züst et al., 2011).

Generally, cap formation requires three successive steps (Fig. 4) (Furuichi et al., 1976): (i) an RNA 5′-triphosphatase (RTPase) hydrolyses the 5′ γ-phosphate of the nascent mRNA; (ii) a guanylyltransferase (GTase) catalyses the transfer of a guanosine monophosphate (GMP) to the diphosphate mRNA 5′ end; (iii) an RNA methyltransferase (MTase) adds a methyl group at the N7 position of the cap guanine. As previously mentioned, CoV cap is a "cap-1", and thus another MTase transfers a methyl group to the 2′O position of the first mRNA nucleotide and this enzyme is so called 2′-O-MTase. As already mentioned, RNA cap methylation is a very important process, "hiding" the viral mRNA from innate immunity sensors but also preventing the pyrophosphorolytic reversal of the

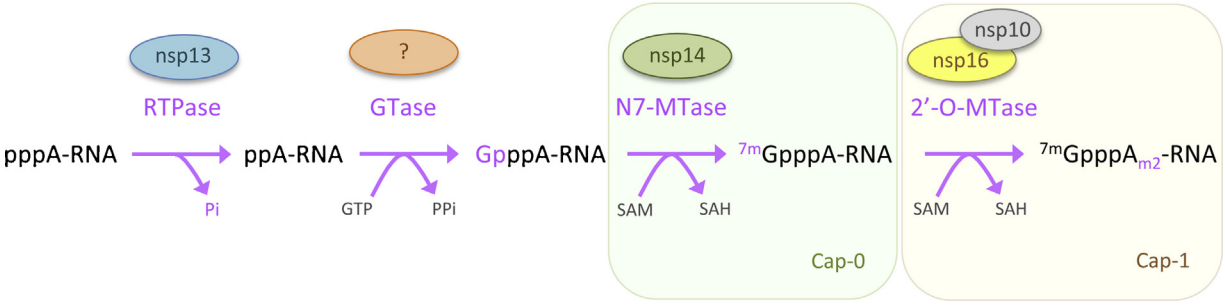

Fig. 4. SARS-CoV RNA capping pathway. SARS-CoV uses a canonical capping pathway. The 5′-end γ-phosphate of the RNA is hydrolyzed by the nsp13 RTPase activity. Then, the still unknown RNA GTase transfers a GMP to the 5′-diphosphate RNA end, forming a 5′–5′ triphosphate bond. Next, the nsp14 N7-MTase transfers a methyl group from the SAM donor to the N7-position of the cap, forming the "cap-0" structure. Lastly, the nsp16/nsp10 2′O-MTase methylates the first RNA nucleotide in the 2′O position, to form the "cap-1" structure.

guanylyltransfer reaction (Furuichi et al., 1977; Shuman, 2001). Knocking-out cap methylation genes in SARS-CoV is lethal if not detrimental for virus replication (Almazán et al., 2006; Chen et al., 2009).

SARS-CoV replicates in the cytoplasm, without access to the nuclear host-cell machinery for mRNA capping. Therefore, SARS-CoV has two options for capping its mRNAs: either the virus can hijack the cellular machinery or it has to produce its own RNA-capping enzymes (Mao and Shuman, 1994). So far, out of the four necessary activities involved in mRNA capping, three were identified in the CoV ORF1b (Figs. 1 and 4) (Subissi et al., 2014a). Current knowledge regarding the 4 steps of cap formation is more fully described in Sections 5.1–5.4. Unless otherwise specified, all data were shown for the SARS-CoV.

5.1. The RNA 5′-triphosphatase (RTPase)

RTPase catalyses the cleavage of the interphosphate bond between the β- and the γ-phosphates at the 5′-end of a triphosphorylated mRNA. Biochemical assays indicate that this function, together with a helicase activity might be played by nsp13 (as described in paragraph 3.1) (Ivanov et al., 2004b). The combination of RTPase and helicase activities carried by the same protein has already been observed for many RNA viruses (Wengler and Wengler, 1993; Bisaillon et al., 1997; Vasiljeva et al., 2000; Li et al., 2001; Benarroch et al., 2004b). Nevertheless, the exact RTPase mechanism as well as the high-resolution structure of nsp13 are still unknown.

5.2. The guanylyltransferase (GTase)

The guanylyltransferase (GTase) enzyme allows the transfer of GMP to the 5′-diphosphate mRNA end (Fig. 4) (Roth and Hurwitz, 1984). Most GTase proteins were shown to create covalent links with GMP before its subsequent transfer onto the diphosphate end of the RNA (Ahola and Ahlquist, 1999).

Many efforts have been made to identify the SARS-CoV GTase, unsuccessfully so far. No GMP covalent link was found for nsp7, nsp8, nsp10/nsp16, nsp12, nsp13, nsp14 or nsp15 (Jin et al., 2013). Yeast trans-complementation experiments, that had allowed discovery of the N7-MTase activity (see Section 5.3), did not allow the identification of the SARS-CoV GTase activity (Chen et al., 2009). This function remains elusive.

5.3. The N7-methyltransferase (N7-MTase)

The methylation of the mRNA at the N7 position of the cap is the third step of cap formation and leads to a "cap-0" (^{7m}GpppN) (Fig. 3). N7-MTases are S-adenosyl-L-methionine (SAM) dependent enzymes. A methyl group is transferred from the SAM to the cap-RNA, producing also S-adenosyl-homocysteine (SAH) as by-product.

Functional screenings in yeast have revealed that SARS-CoV nsp14 is able to complement the deletion of the cellular cap N7-MTase (Chen et al., 2009). Furthermore, this activity was demonstrated by biochemical analysis. Nsp14 is able to methylate the N7 position in presence of SAM without any sequence specificity (Chen et al., 2009; Bouvet et al., 2010). Indeed, nsp14 N7-MTase is active on different types of substrates: GTP and dGTP as well as cap analogs (GpppG, GpppA and ^{m7}GpppG) (Jin et al., 2013). By sequence alignment and comparison of conserved motifs, the N7-MTase activity was attributed to the C-terminal domain of nsp14. Biochemical analysis revealed that both nsp14 enzymatic activities (ExoN and N7-MTase) are functionally distinct. However, based on deletion mutation analysis the two functional domains seem structurally linked (Chen et al., 2009) and a large region of nsp14 (aa 62 to 527) is essential for both N7-MTase and ExoN activities. The N7-MTase activity is strongly dependent on the N-terminal domain. However, the N-terminal ExoN domain is not involved in substrate binding for the N7-MTase activity (Chen et al., 2013). Nsp10, which was shown to strongly enhance the nsp14 ExoN activity (Bouvet et al., 2012), has no effect on the nsp14 N7-MTase activity (Bouvet et al., 2010).

The most conserved motif among N7-MTases is the SAM-binding site with a specific sequence signature "D/ExGxGxG" (where x refers to any amino acid) (Martin and McMillan, 2002). According to CoV nsp14 sequence alignments, the motif DxGx-PxG/A (aa 331 to 337) may represent the SAM-binding site of the nsp14 N7-MTase (Chen et al., 2009; Bouvet et al., 2010). Moreover, two more regions, the first ranging from aa 310 to 428, overlapping with the core domain of N7-MTase, and the second ranging from aa 73 to 86, located at the N-terminus of the ExoN domain were found to be essential for nsp14 N7-MTase activity (Chen et al., 2013).

The SAM-dependent MTase family exhibits low sequence conservation but possesses a highly conserved structural fold, named Rossmann-like fold (Martin and McMillan, 2002; Schubert et al., 2003). This fold is an alternation of β-stranded and α-helical regions, with 7 strands forming a central relatively planar β-sheet and a varying number of helices creating two layers, one on each side of the plane (Martin and McMillan, 2002). Based on the known structure of mRNA cap N7-MTase, a structural model of SARS-CoV nsp14 core N7-MTase was created (Chen et al., 2013). This model confirmed the implication of DxGxPxG/A motif in SAM binding. Nevertheless, the determination of the full-length nsp14 structure is required to better understand the functional mechanism of the N7-MTase activity.

5.4. The 2′-O-methyltransferase (2′-O-MTase)

A 2′-O-MTase transfers a methyl group from the SAM methyl donor to the first mRNA nucleotide. This step converts the "cap-0" to a "cap-1" structure ($^{7m}Gppp_{m2}N$), this last form being found in all higher eukaryotes (Fig. 3). Lower eukaryotes, including yeast, employ usually a "cap-0" ($^{7m}GpppN$) structure. Many RNA viruses have evolved to adopt the "cap-1" structure, yielding to "cellular-like mRNA". Züst et al. (2011) highlighted a biological role for viral mRNA 2′-O-methylation. They showed that 2′-O-methylation subverts the induction of type I interferon, acting as a molecular signature to distinguish self and non-self mRNA.

2′-O-MTases belong to the same family as N7-MTase, with low sequence identity but a common Rossmann-like structural fold (see section 5.3) encompassing the canonical catalytic tetrad K-D-K-E (Bujnicki and Rychlewski, 2001; Ferron et al., 2002; Benarroch et al., 2004a). The functional mechanism of the vaccinia virus (vv) 2′-O-MTase VP39 has been extensively described (Hodel et al., 1996; Lockless et al., 1998). The reaction mechanism seems to involve a bi-molecular nucleophilic substitution (S_N2 type) in which the nucleophilic ribose 2′-hydroxyl group of a lysine attacks the SAM methyl group, thus leading to the release of SAH (Li et al., 2004).

Bioinformatics studies on the SARS-CoV have predicted a SAM-dependent 2′-O-MTase harbored by nsp16 (Von Grotthuss et al., 2003). This activity was confirmed *in vitro* for FCoV nsp16 (Decroly et al., 2008) and, with a lower activity for SARS-CoV nsp16. Bouvet et al. (2010) showed evidences that SARS-CoV nsp16 2′-O-MTase activity is stimulated by the addition of nsp10 through direct protein/protein interaction. They found out that the nsp10/nsp16 complex can methylate the 2′O position of the first mRNA nucleotide only if the cap is already methylated at the N7 position. Using a mutational approach, K_{46}-D_{130}-K_{170}-E_{203} residues were identified as the catalytic tetrad (Fig. 5). The 2′-O-MTase activity is completely abolished by any single mutation of this catalytic tetrad, demonstrating that although nsp10 stimulates the nsp16 2′-O-MTase activity, the catalytic site itself resides in nsp16 (Bouvet et al., 2010). Noteworthy, a similar activation of MTase activity was previously reported for the vaccinia virus capping enzyme (Mao and Shuman, 1994). The structure of the co-factor nsp10 was first solved and revealed a novel fold with a pair of antiparallel N-terminal α-helices stacked against an irregular β-sheet, a coil-rich C-terminus and two Zn fingers (Joseph et al., 2006; Su et al., 2006). The crystal structure of SARS-CoV nsp16 in complex with nsp10 was determined in 2011 by 2 groups (Fig. 5) (Chen et al., 2011; Decroly et al., 2011). The nsp10 overall structure in complex with nsp16 remains quite similar to the one determined for the free nsp10. Nsp16 adopts a canonical SAM-dependent MTase fold with two binding domains, one for the methyl donor SAM and another for the methyl acceptor substrate (capped-RNA). Nsp16 fold is a central β-sheet of 7 strands surrounded by five α-helices. Compared to the MTase canonical fold, two α-helices are absent in the SAM binding region of nsp16, but the complex formed with nsp10 seems to compensate and stabilize the overall structure of nsp16. Whereas earlier reports claimed that Mg^{2+} was necessary for the nsp10/nsp16 2′-O-MTase activity (Bouvet et al., 2010), no cation was observed in the active site. However, the structure shows a Mg^{2+} located far from the SAM-binding site (Fig. 5). It is thus possible that divalent cations play a structural role in the nsp16 structure in stabilizing the general fold. The organization of the active site is in agreement with the current 2′-O-MTase mechanism described above, transferring the methyl group of SAM to capped-RNA. Although no RNA-bound structure is available to date, a putative RNA-binding groove was proposed based on the highly positively charged patch found on nsp16 at the proximity of the catalytic site (Fig. 6) (Chen et al., 2011; Decroly et al., 2011).

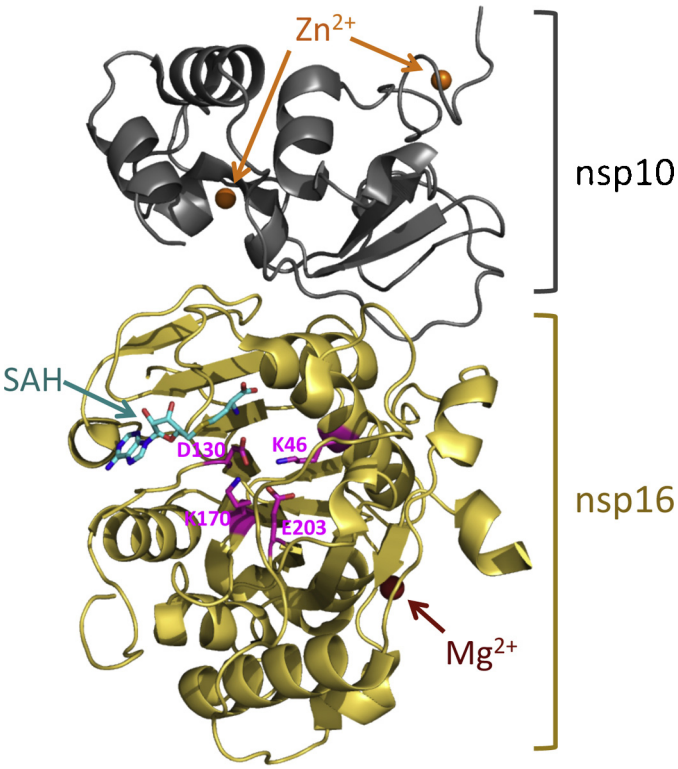

Fig. 5. Crystal structure of SARS-CoV nsp10/nsp16 complex. Ribbon representation of nsp10 (in gray) in complex with nsp16 (in yellow) (from Decroly et al., 2011; PDB 2XYQ). Mg^{2+} ion (in brown) found on nsp16 is localized at the opposite side of the 2′O-MTase active site which is formed by the catalytic tetrad K46, D130, K170 and E203 (in pink). The by-product of the reaction, SAH in cyan is localized near the catalytic site. The two Zn^{2+} ions (orange) on nsp10 are not involved in the interaction with nsp16.

Nsp10 alone does not exhibit any enzyme activity but appears to be central for two distinct regulatory mechanisms (nsp14 ExoN and nsp16 2′-O-MTase). Our group has determined the interaction surface of nsp10 with nsp14 and with nsp16 (Bouvet et al., 2014; Lugari et al., 2010). These studies show that the same nsp10 interface is involved in complex formation with both nsp16 and nsp14.

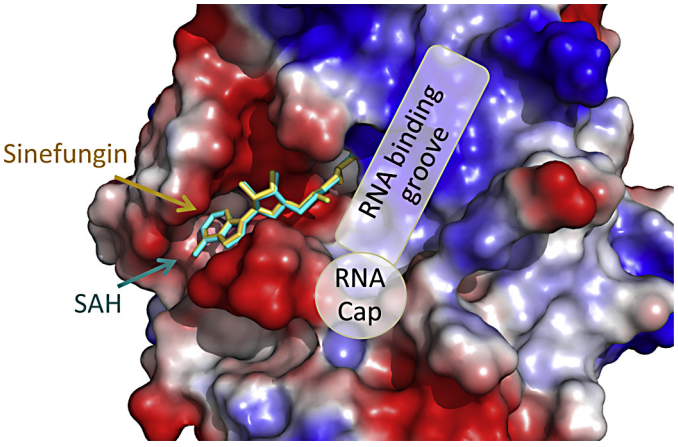

Fig. 6. Sinefungin binding site and hypothetical RNA binding groove on SARS-CoV nsp16. Electrostatic potential surface of nsp16 presented with SAH (in cyan) and sinefungin (in yellow), which are localized in the same pocket. A putative binding groove for a capped-mRNA is indicated.

Source: From Decroly et al. (2011) and Chen et al. (2011); PDB codes 2XYQ and 2XYV.

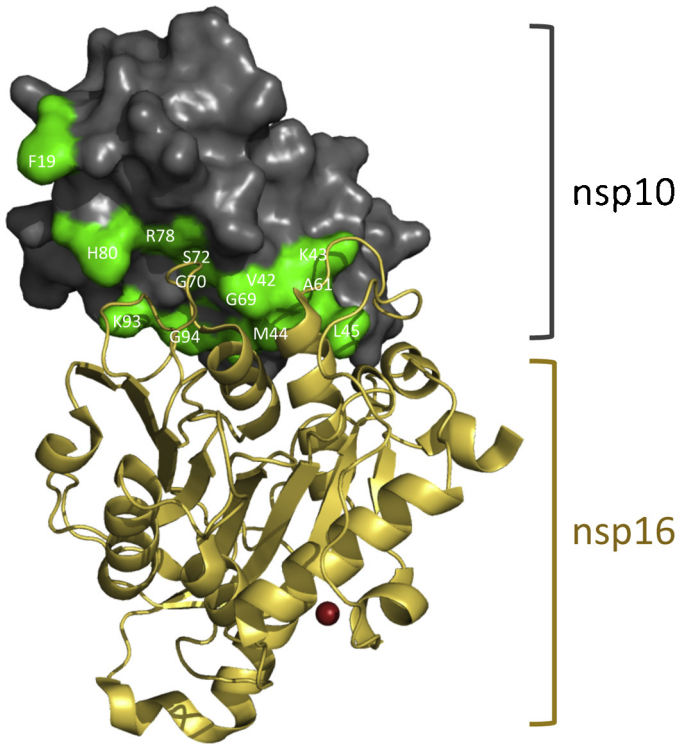

Fig. 7. Comparison of SARS-CoV nsp10 interaction surface with nsp14 and with nsp16. The SARS-CoV nsp10/nsp16 complex structure is presented with nsp10 solvent-accessible surface in gray, and nsp16 in yellow ribbon. Nsp10 residues involved in the interaction with nsp14 are depicted in green. The interaction surface of nsp10 with nsp16 and nsp14 overlaps, the latter being wider (Bouvet et al., 2014).

However, in the case of nsp10/nsp14, the interaction interface is substantially wider (Fig. 7). As a consequence, nsp10 cannot interact simultaneously with both nsp14 and nsp16. Nevertheless, the two regulatory functions of nsp10 may still act simultaneously, since nsp10 is translated in stoichiometric excess compared to ORF1b-encoded nsp14 and nsp16 (Fig. 1) (Snijder et al., 2003).

Eukaryotic and viral mRNA capping systems show many differences (Furuichi and Shatkin, 2000), and given the essential role fulfilled by these systems, each protein involved in this process should be considered as a potential antiviral target. In particular, viral MTases seem to be good candidates (Dong et al., 2008; Bollati et al., 2010; Dong et al., 2010). Indeed, mutations abolishing MTase activities have a detrimental effect on viral replication (Almazán et al., 2006; Ray et al., 2006; Chen et al., 2009). *In vitro*, sinefungin and SAH (the by-product of the methyl transfer reaction) were found to inhibit both SARS-CoV MTase activities (Bouvet et al., 2010). Furthermore, a crystal structure of the SARS-CoV nsp10/nsp16 complex with sinefungin was solved and revealed that the molecule is bound in the SAM-binding pocket and hence should inhibit nsp16 2′-O-MTase activity (Fig. 6). In addition, aurintricarboxylic acid (ATA), expected to bind MTase active site, inhibits SARS-CoV replication (He et al., 2004; Milani et al., 2009). Biochemical assays demonstrated that ATA inhibits both nsp14 N7-MTase and nsp16 2′-O-MTase activities (Bouvet et al., 2010). Recently, Sun et al. (2014) developed a yeast-based high-throughput antiviral screening system to find novel anti-coronavirus drugs. This study confirmed that sinefungin significantly suppresses the growth of yeast cells complemented with nsp14 N7-MTase gene. However, sinefungin is not a specific inhibitor as it also inhibits yeast and human MTases (Sun et al., 2014).

6. Conclusion

Coronaviruses have only recently attracted a wider audience due to public health issues generated by SARS- and MERS-CoV emergences. However, remarkable achievements have been made regarding the elucidation of structures, functions, and mechanisms of what appears to be the most sophisticated and regulated (+) RNA genome replication/transcription machinery so far. Although other viruses, such as Hepatitis C and Influenza viruses, might be better and sooner controlled through antiviral therapies, the study of coronaviruses may well accelerate our current understanding of RNA synthesis, evolution, capping, repair, as well as all novel implications arising from the combination and coordination of these RNA processing activities. Further experiments should open an entirely new field of research, since for viral RNA synthesis, very few data are available on these processes. For example, it is possible to quantitate mismatch formation for some RNA viruses (Hepatitis C Virus (Powdrill et al., 2011), Poliovirus (Korneeva and Cameron, 2007), Dengue virus (Jin et al., 2011)) and sometimes only for a restricted set of nucleotides (Dengue virus (Jin et al., 2011)).

The progress made on SARS-CoV RNA synthesis machinery comprehension will soon allow to measure, through genome sequencing, the RNA replication fidelity. This knowledge will likely open a Pandora box containing the coronavirus “playbook” exposing how they maintain the integrity of their large genomes, while generating the population diversity required for emergence and adaptation. Knowing in detail these mechanisms will provide new antiviral strategies.

Acknowledgements

We thank Barbara Selisko for her critical reading. This work was supported by the French National Research Agency, under references “ANR-08-MIEN-032 and ANR-12-BSV3”, and by the European Union Seventh Framework Program through the project SILVER (Small Inhibitor Leads Versus Emerging and Neglected RNA viruses, Grant Agreement N° 260644). LS had a Marie Curie Fellowship through the EUVIRNA project.

References

Adedeji, A.O., Marchand, B., Te Velthuis, A.J.W., Snijder, E.J., Weiss, S., Eoff, R.L., Singh, K., Sarafianos, S.G., 2012. Mechanism of nucleic acid unwinding by SARS-CoV helicase. PLOS ONE 7, e36521, http://dx.doi.org/10.1371/journal.pone.0036521.

Ahola, T., Ahlquist, P., 1999. Putative RNA capping activities encoded by brome mosaic virus: methylation and covalent binding of guanylate by replicase protein 1a. J. Virol. 73, 10061–10069.

Almazán, F., Dediego, M.L., Galán, C., Escors, D., Alvarez, E., Ortego, J., Sola, I., Zuñiga, S., Alonso, S., Moreno, J.L., Nogales, A., Capiscol, C., Enjuanes, L., 2006. Construction of a severe acute respiratory syndrome coronavirus infectious cDNA clone and a replicon to study coronavirus RNA synthesis. J. Virol. 80, 10900–10906, http://dx.doi.org/10.1128/JVI.00385-06.

Azhar, E.I., El-Kafrawy, S.A., Farraj, S.A., Hassan, A.M., Al-Saeed, M.S., Hashem, A.M., Madani, T.A., 2014. Evidence for camel-to-human transmission of MERS coronavirus. N. Engl. J. Med. 370, 2499–2505, http://dx.doi.org/10.1056/NEJMoa1401505.

Benarroch, D., Egloff, M.-P., Mulard, L., Guerreiro, C., Romette, J.-L., Canard, B., 2004a. A structural basis for the inhibition of the NS5 dengue virus mRNA 2′-O-methyltransferase domain by ribavirin 5′-triphosphate. J. Biol. Chem. 279, 35638–35643, http://dx.doi.org/10.1074/jbc.M400460200.

Benarroch, D., Selisko, B., Locatelli, G.A., Maga, G., Romette, J.-L., Canard, B., 2004b. The RNA helicase, nucleotide 5′-triphosphatase, and RNA 5′-triphosphatase activities of Dengue virus protein NS3 are Mg^{2+}-dependent and require a functional Walker B motif in the helicase catalytic core. Virology 328, 208–218, http://dx.doi.org/10.1016/j.virol.2004.07.004.

Bisaillon, M., Bergeron, J., Lemay, G., 1997. Characterization of the nucleoside triphosphate phosphohydrolase and helicase activities of the reovirus lambda1 protein. J. Biol. Chem. 272, 18298–18303.

Bollati, M., Alvarez, K., Assenberg, R., Baronti, C., Canard, B., Cook, S., Coutard, B., Decroly, E., de Lamballerie, X., Gould, E.A., Grard, G., Grimes, J.M., Hilgenfeld, R., Jansson, A.M., Malet, H., Mancini, E.J., Mastrangelo, E., Mattevi, A., Milani, M., Moureau, G., Neyts, J., Owens, R.J., Ren, J., Selisko, B., Speroni, S., Steuber, H., Stuart, D.I., Unge, T., Bolognesi, M., 2010. Structure and functionality in

flavivirus NS-proteins: perspectives for drug design. Antiviral Res. 87, 125–148, http://dx.doi.org/10.1016/j.antiviral.2009.11.009.
Bouvet, M., Debarnot, C., Imbert, I., Selisko, B., Snijder, E.J., Canard, B., Decroly, E., 2010. In vitro reconstitution of SARS-coronavirus mRNA cap methylation. PLoS Pathog. 6, e1000863, http://dx.doi.org/10.1371/journal.ppat.1000863.
Bouvet, M., Imbert, I., Subissi, L., Gluais, L., Canard, B., Decroly, E., 2012. RNA 3′-end mismatch excision by the severe acute respiratory syndrome coronavirus nonstructural protein nsp10/nsp14 exoribonuclease complex. Proc. Natl. Acad. Sci. U. S. A. 109, 9372–9377, http://dx.doi.org/10.1073/pnas.1201130109.
Bouvet, M., Lugari, A., Posthuma, C.C., Zevenhoven, J.C., Bernard, S., Betzi, S., Imbert, I., Canard, B., Guillemot, J.-C., Lécine, P., Pfefferle, S., Drosten, C., Snijder, E.J., Decroly, E., Morelli, X., 2014. Coronavirus Nsp10: a critical co-factor for activation of multiple replicative enzymes. J. Biol. Chem., http://dx.doi.org/10.1074/jbc.M114.577353.
Bujnicki, J.M., Rychlewski, L., 2001. Reassignment of specificities of two cap methyltransferase domains in the reovirus lambda 2 protein. Genome Biol. 2 (RESEARCH0038).
Cheng, A., Zhang, W., Xie, Y., Jiang, W., Arnold, E., Sarafianos, S.G., Ding, J., 2005. Expression, purification, and characterization of SARS coronavirus RNA polymerase. Virology 335, 165–176, http://dx.doi.org/10.1016/j.virol.2005.02.017.
Chen, Y., Cai, H., Pan, J., Xiang, N., Tien, P., Ahola, T., Guo, D., 2009. Functional screen reveals SARS coronavirus nonstructural protein nsp14 as a novel cap N7 methyltransferase. Proc. Natl. Acad. Sci. U. S. A. 106, 3484–3489, http://dx.doi.org/10.1073/pnas.0808790106.
Chen, Y., Su, C., Ke, M., Jin, X., Xu, L., Zhang, Z., Wu, A., Sun, Y., Yang, Z., Tien, P., Ahola, T., Liang, Y., Liu, X., Guo, D., 2011. Biochemical and structural insights into the mechanisms of SARS coronavirus RNA ribose 2′-O-methylation by nsp16/nsp10 protein complex. PLoS Pathog. 7, e1002294, http://dx.doi.org/10.1371/journal.ppat.1002294.
Chen, Y., Tao, J., Sun, Y., Wu, A., Su, C., Gao, G., Cai, H., Qiu, S., Wu, Y., Ahola, T., Guo, D., 2013. Structure-function analysis of severe acute respiratory syndrome coronavirus RNA cap guanine-N7-methyltransferase. J. Virol. 87, 6296–6305, http://dx.doi.org/10.1128/JVI.00061-13.
Decroly, E., Debarnot, C., Ferron, F., Bouvet, M., Coutard, B., Imbert, I., Gluais, L., Papageorgiou, N., Sharff, A., Bricogne, G., Ortiz-Lombardia, M., Lescar, J., Canard, B., 2011. Crystal structure and functional analysis of the SARS-coronavirus RNA cap 2′-O-methyltransferase nsp10/nsp16 complex. PLoS Pathog. 7, e1002059, http://dx.doi.org/10.1371/journal.ppat.1002059.
Decroly, E., Ferron, F., Lescar, J., Canard, B., 2012. Conventional and unconventional mechanisms for capping viral mRNA. Nat. Rev. Microbiol. 10, 51–65, http://dx.doi.org/10.1038/nrmicro2675.
Decroly, E., Imbert, I., Coutard, B., Bouvet, M., Selisko, B., Alvarez, K., Gorbalenya, A.E., Snijder, E.J., Canard, B., 2008. Coronavirus nonstructural protein 16 is a cap-0 binding enzyme possessing (nucleoside-2′O)-methyltransferase activity. J. Virol. 82, 8071–8084, http://dx.doi.org/10.1128/JVI.00407-08.
De Groot, R.J., Baker, S.C., Baric, R.S., Brown, C.S., Drosten, C., Enjuanes, L., Fouchier, R.A.M., Galiano, M., Gorbalenya, A.E., Memish, Z.A., Perlman, S., Poon, L.L.M., Snijder, E.J., Stephens, G.M., Woo, P.C.Y., Zaki, A.M., Zambon, M., Ziebuhr, J., 2013. Middle East respiratory syndrome coronavirus (MERS-CoV): announcement of the Coronavirus Study Group. J. Virol. 87, 7790–7792, http://dx.doi.org/10.1128/JVI.01244-13.
Dong, H., Liu, L., Zou, G., Zhao, Y., Li, Z., Lim, S.P., Shi, P.-Y., Li, H., 2010. Structural and functional analyses of a conserved hydrophobic pocket of flavivirus methyltransferase. J. Biol. Chem. 285, 32586–32595, http://dx.doi.org/10.1074/jbc.M110.129197.
Dong, H., Zhang, B., Shi, P.-Y., 2008. Flavivirus methyltransferase: a novel antiviral target. Antiviral Res. 80, 1–10, http://dx.doi.org/10.1016/j.antiviral.2008.05.003.
Eckerle, L.D., Becker, M.M., Halpin, R.A., Li, K., Venter, E., Lu, X., Scherbakova, S., Graham, R.L., Baric, R.S., Stockwell, T.B., Spiro, D.J., Denison, M.R., 2010. Infidelity of SARS-CoV Nsp14-exonuclease mutant virus replication is revealed by complete genome sequencing. PLoS Pathog. 6, e1000896, http://dx.doi.org/10.1371/journal.ppat.1000896.
Eckerle, L.D., Lu, X., Sperry, S.M., Choi, L., Denison, M.R., 2007. High fidelity of murine hepatitis virus replication is decreased in nsp14 exoribonuclease mutants. J. Virol. 81, 12135–12144, http://dx.doi.org/10.1128/JVI.01296-07.
Egloff, M.-P., Ferron, F., Campanacci, V., Longhi, S., Rancurel, C., Dutartre, H., Snijder, E.J., Gorbalenya, A.E., Cambillau, C., Canard, B., 2004. The severe acute respiratory syndrome-coronavirus replicative protein nsp9 is a single-stranded RNA-binding subunit unique in the RNA virus world. Proc. Natl. Acad. Sci. U. S. A. 101, 3792–3796, http://dx.doi.org/10.1073/pnas.0307877101.
Ferron, F., Longhi, S., Henrissat, B., Canard, B., 2002. Viral RNA-polymerases – a predicted 2′-O-ribose methyltransferase domain shared by all Mononegavirales. Trends Biochem. Sci. 27, 222–224.
Furuichi, Y., LaFiandra, A., Shatkin, A.J., 1977. 5′-Terminal structure and mRNA stability. Nature 266, 235–239.
Furuichi, Y., Muthukrishnan, S., Tomasz, J., Shatkin, A.J., 1976. Mechanism of formation of reovirus mRNA 5′-terminal blocked and methylated sequence, m7GpppGmpC. J. Biol. Chem. 251, 5043–5053.
Furuichi, Y., Shatkin, A.J., 2000. Viral and cellular mRNA capping: past and prospects. Adv. Virus Res. 55, 135–184.
Ge, X.-Y., Li, J.-L., Yang, X.-L., Chmura, A.A., Zhu, G., Epstein, J.H., Mazet, J.K., Hu, B., Zhang, W., Peng, C., Zhang, Y.-J., Luo, C.-M., Tan, B., Wang, N., Zhu, Y., Crameri, G., Zhang, S.-Y., Wang, L.-F., Daszak, P., Shi, Z.-L., 2013. Isolation and characterization of a bat SARS-like coronavirus that uses the ACE2 receptor. Nature 503, 535–538, http://dx.doi.org/10.1038/nature12711.
Gorbalenya, A.E., Enjuanes, L., Ziebuhr, J., Snijder, E.J., 2006. Nidovirales: evolving the largest RNA virus genome. Virus Res. 117, 17–37, http://dx.doi.org/10.1016/j.virusres.2006.01.017.
Gorbalenya, A.E., Pringle, F.M., Zeddam, J.-L., Luke, B.T., Cameron, C.E., Kalmakoff, J., Hanzlik, T.N., Gordon, K.H.J., Ward, V.K., 2002. The palm subdomain-based active site is internally permuted in viral RNA-dependent RNA polymerases of an ancient lineage. J. Mol. Biol. 324, 47–62.
Hastie, K.M., Kimberlin, C.R., Zandonatti, M.A., MacRae, I.J., Saphire, E.O., 2011. Structure of the Lassa virus nucleoprotein reveals a dsRNA-specific 3′ to 5′ exonuclease activity essential for immune suppression. Proc. Natl. Acad. Sci. U. S. A. 108, 2396–2401, http://dx.doi.org/10.1073/pnas.1016404108.
He, R., Adonov, A., Traykova-Adonova, M., Cao, J., Cutts, T., Grudesky, E., Deschambaul, Y., Berry, J., Drebot, M., Li, X., 2004. Potent and selective inhibition of SARS coronavirus replication by aurintricarboxylic acid. Biochem. Biophys. Res. Commun. 320, 1199–1203, http://dx.doi.org/10.1016/j.bbrc.2004.06.076.
Hodel, A.E., Gershon, P.D., Shi, X., Quiocho, F.A., 1996. The 1.85 A structure of vaccinia protein VP39: a bifunctional enzyme that participates in the modification of both mRNA ends. Cell 85, 247–256.
Imbert, I., Guillemot, J.-C., Bourhis, J.-M., Bussetta, C., Coutard, B., Egloff, M.-P., Ferron, F., Gorbalenya, A.E., Canard, B., 2006. A second, non-canonical RNA-dependent RNA polymerase in SARS coronavirus. EMBO J. 25, 4933–4942, http://dx.doi.org/10.1038/sj.emboj.7601368.
Imbert, I., Snijder, E.J., Dimitrova, M., Guillemot, J.-C., Lécine, P., Canard, B., 2008. The SARS-Coronavirus PLnc domain of nsp3 as a replication/transcription scaffolding protein. Virus Res. 133, 136–148, http://dx.doi.org/10.1016/j.virusres.2007.11.017.
Ivanov, K.A., Hertzig, T., Rozanov, M., Bayer, S., Thiel, V., Gorbalenya, A.E., Ziebuhr, J., 2004a. Major genetic marker of nidoviruses encodes a replicative endoribonuclease. Proc. Natl. Acad. Sci. U. S. A. 101, 12694–12699, http://dx.doi.org/10.1073/pnas.0403127101.
Ivanov, K.A., Thiel, V., Dobbe, J.C., van der Meer, Y., Snijder, E.J., Ziebuhr, J., 2004b. Multiple enzymatic activities associated with severe acute respiratory syndrome coronavirus helicase. J. Virol. 78, 5619–5632, http://dx.doi.org/10.1128/JVI.78.11.5619-5632.2004.
Jin, X., Chen, Y., Sun, Y., Zeng, C., Wang, Y., Tao, J., Wu, A., Yu, X., Zhang, Z., Tian, J., Guo, D., 2013. Characterization of the guanine-N7 methyltransferase activity of coronavirus nsp14 on nucleotide GTP. Virus Res. 176, 45–52, http://dx.doi.org/10.1016/j.virusres.2013.05.001.
Jin, Z., Deval, J., Johnson, K.A., Swinney, D.C., 2011. Characterization of the elongation complex of dengue virus RNA polymerase: assembly, kinetics of nucleotide incorporation, and fidelity. J. Biol. Chem. 286, 2067–2077, http://dx.doi.org/10.1074/jbc.M110.162685.
Joseph, J.S., Saikatendu, K.S., Subramanian, V., Neuman, B.W., Brooun, A., Griffith, M., Moy, K., Yadav, M.K., Velasquez, J., Buchmeier, M.J., Stevens, R.C., Kuhn, P., 2006. Crystal structure of nonstructural protein 10 from the severe acute respiratory syndrome coronavirus reveals a novel fold with two zinc-binding motifs. J. Virol. 80, 7894–7901, http://dx.doi.org/10.1128/JVI.00467-06.
Knoops, K., Kikkert, M., van den Worm, S.H.E., Zevenhoven-Dobbe, J.C., van der Meer, Y., Koster, A.J., Mommaas, A.M., Snijder, E.J., 2008. SARS-coronavirus replication is supported by a reticulovesicular network of modified endoplasmic reticulum. PLoS Biol. 6, e226, http://dx.doi.org/10.1371/journal.pbio.0060226.
Korneeva, V.S., Cameron, C.E., 2007. Structure-function relationships of the viral RNA-dependent RNA polymerase: fidelity, replication speed, and initiation mechanism determined by a residue in the ribose-binding pocket. J. Biol. Chem. 282, 16135–16145, http://dx.doi.org/10.1074/jbc.M610090200.
Lai, M.M., Stohlman, S.A., 1981. Comparative analysis of RNA genomes of mouse hepatitis viruses. J. Virol. 38, 661–670.
Lee, N.-R., Kwon, H.-M., Park, K., Oh, S., Jeong, Y.-J., Kim, D.-E., 2010. Cooperative translocation enhances the unwinding of duplex DNA by SARS coronavirus helicase nsP13. Nucleic Acids Res. 38, 7626–7636, http://dx.doi.org/10.1093/nar/gkq647.
Li, C., Xia, Y., Gao, X., Gershon, P.D., 2004. Mechanism of RNA 2′-O-methylation: evidence that the catalytic lysine acts to steer rather than deprotonate the target nucleophile. Biochemistry (Mosc.) 43, 5680–5687, http://dx.doi.org/10.1021/bi0359980.
Li, W., Shi, Z., Yu, M., Ren, W., Smith, C., Epstein, J.H., Wang, H., Crameri, G., Hu, Z., Zhang, H., Zhang, J., McEachern, J., Field, H., Daszak, P., Eaton, B.T., Zhang, S., Wang, L.-F., 2005. Bats are natural reservoirs of SARS-like coronaviruses. Science 310, 676–679, http://dx.doi.org/10.1126/science.1118391.
Li, Y.I., Shih, T.W., Hsu, Y.H., Han, Y.T., Huang, Y.L., Meng, M., 2001. The helicase-like domain of plant potexvirus replicase participates in formation of RNA 5′ cap structure by exhibiting RNA 5′-triphosphatase activity. J. Virol. 75, 12114–12120, http://dx.doi.org/10.1128/JVI.75.24.12114-12120.2001.
Lockless, S.W., Cheng, H.T., Hodel, A.E., Quiocho, F.A., Gershon, P.D., 1998. Recognition of capped RNA substrates by VP39, the vaccinia virus-encoded mRNA cap-specific 2′-O-methyltransferase. Biochemistry (Mosc.) 37, 8564–8574, http://dx.doi.org/10.1021/bi980178m.
Lugari, A., Betzi, S., Decroly, E., Bonnaud, E., Hermant, A., Guillemot, J.-C., Debarnot, C., Borg, J.-P., Bouvet, M., Canard, B., Morelli, X., Lécine, P., 2010. Molecular mapping of the RNA Cap 2′-O-methyltransferase activation interface between severe acute respiratory syndrome coronavirus nsp10 and nsp16. J. Biol. Chem. 285, 33230–33241, http://dx.doi.org/10.1074/jbc.M110.120014.
Mao, X., Shuman, S., 1994. Intrinsic RNA (guanine-7) methyltransferase activity of the vaccinia virus capping enzyme D1 subunit is stimulated by the D12 subunit, Identification of amino acid residues in the D1 protein required for subunit association and methyl group transfer. J. Biol. Chem. 269, 24472–24479.

Martin, J.L., McMillan, F.M., 2002. SAM (dependent) I AM: the S-adenosylmethionine-dependent methyltransferase fold. Curr. Opin. Struct. Biol. 12, 783–793.
Miknis, Z.J., Donaldson, E.F., Umland, T.C., Rimmer, R.A., Baric, R.S., Schultz, L.W., 2009. Severe acute respiratory syndrome coronavirus nsp9 dimerization is essential for efficient viral growth. J. Virol. 83, 3007–3018, http://dx.doi.org/10.1128/JVI.01505-08.
Milani, M., Mastrangelo, E., Bollati, M., Selisko, B., Decroly, E., Bouvet, M., Canard, B., Bolognesi, M., 2009. Flaviviral methyltransferase/RNA interaction: structural basis for enzyme inhibition. Antiviral Res. 83, 28–34, http://dx.doi.org/10.1016/j.antiviral.2009.03.001.
Minskaia, E., Hertzig, T., Gorbalenya, A.E., Campanacci, V., Cambillau, C., Canard, B., Ziebuhr, J., 2006. Discovery of an RNA virus 3′ → 5′ exoribonuclease that is critically involved in coronavirus RNA synthesis. Proc. Natl. Acad. Sci. U. S. A. 103, 5108–5113, http://dx.doi.org/10.1073/pnas.0508200103.
Pasternak, A.O., Spaan, W.J.M., Snijder, E.J., 2006. Nidovirus transcription: how to make sense…? J. Gen. Virol. 87, 1403–1421, http://dx.doi.org 10.1099/vir.0.81611-0.
Perera, R., Wang, P., Gomaa, M., El-Shesheny, R., Kandeil, A., Bagato, O., Siu, L., Shehata, M., Kayed, A., Moatasim, Y., Li, M., Poon, L., Guan, Y., Webby, R., Ali, M., Peiris, J., Kayali, G., 2013. Seroepidemiology for MERS coronavirus using microneutralisation and pseudoparticle virus neutralisation assays reveal a high prevalence of antibody in dromedary camels in Egypt, June 2013. Euro Surveill. Bull. Eur. Sur Mal. Transm. Eur. Commun. Dis. Bull., 18.
Poch, O., Sauvaget, I., Delarue, M., Tordo, N., 1989. Identification of four conserved motifs among the RNA-dependent polymerase encoding elements. EMBO J. 8, 3867–3874.
Powdrill, M.H., Tchesnokov, E.P., Kozak, R.A., Russell, R.S., Martin, R., Svarovskaia, E.S., Mo, H., Kouyos, R.D., Götte, M., 2011. Contribution of a mutational bias in hepatitis C virus replication to the genetic barrier in the development of drug resistance. Proc. Natl. Acad. Sci. U. S. A. 108, 20509–20513, http://dx.doi.org/10.1073/pnas.1105797108.
Prelich, G., Tan, C.K., Kostura, M., Mathews, M.B., So, A.G., Downey, K.M., Stillman, B., 1987. Functional identity of proliferating cell nuclear antigen and a DNA polymerase-delta auxiliary protein. Nature 326, 517–520, http://dx.doi.org/10.1038/326517a0.
Ray, D., Shah, A., Tilgner, M., Guo, Y., Zhao, Y., Dong, H., Deas, T.S., Zhou, Y., Li, H., Shi, P.-Y., 2006. West Nile virus 5′-cap structure is formed by sequential guanine N-7 and ribose 2′-O methylations by nonstructural protein 5. J. Virol. 80, 8362–8370, http://dx.doi.org/10.1128/JVI.00814-06.
Reusken, C.B., Haagmans, B.L., Müller, M.A., Gutierrez, C., Godeke, G.-J., Meyer, B., Muth, D., Raj, V.S., Vries, L.S.-D., Corman, V.M., Drexler, J.-F., Smits, S.L., El Tahir, Y.E., De Sousa, R., van Beek, J., Nowotny, N., van Maanen, K., Hidalgo-Hermoso, E., Bosch, B.-J., Rottier, P., Osterhaus, A., Gortázar-Schmidt, C., Drosten, C., Koopmans, M.P., 2013. Middle East respiratory syndrome coronavirus neutralising serum antibodies in dromedary camels: a comparative serological study. Lancet Infect. Dis. 13, 859–866, http://dx.doi.org/10.1016/S1473-3099(13)70164-6.
Roth, M.J., Hurwitz, J., 1984. RNA capping by the vaccinia virus guanylyltransferase. Structure of enzyme-guanylate intermediate. J. Biol. Chem. 259, 13488–13494.
Schubert, H.L., Blumenthal, R.M., Cheng, X., 2003. Many paths to methyltransfer: a chronicle of convergence. Trends Biochem. Sci. 28, 329–335, http://dx.doi.org/10.1016/S0968-0004(03)00090-2.
Seybert, A., Posthuma, C.C., van Dinten, L.C., Snijder, E.J., Gorbalenya, A.E., Ziebuhr, J., 2005. A complex zinc finger controls the enzymatic activities of nidovirus helicases. J. Virol. 79, 696–704, http://dx.doi.org/10.1128/JVI.79.2.696-704.2005.
Shuman, S., 2001. Structure, mechanism, and evolution of the mRNA capping apparatus. Prog. Nucleic Acid Res. Mol. Biol. 66, 1–40.
Smith, E.C., Blanc, H., Vignuzzi, M., Denison, M.R., 2013. Coronaviruses lacking exoribonuclease activity are susceptible to lethal mutagenesis: evidence for proofreading and potential therapeutics. PLoS Pathog. 9, e1003565, http://dx.doi.org/10.1371/journal.ppat.1003565.
Snijder, E.J., Bredenbeek, P.J., Dobbe, J.C., Thiel, V., Ziebuhr, J., Poon, L.L.M., Guan, Y., Rozanov, M., Spaan, W.J.M., Gorbalenya, A.E., 2003. Unique and conserved features of genome and proteome of SARS-coronavirus, an early split-off from the coronavirus group 2 lineage. J. Mol. Biol. 331, 991–1004.
Stadler, K., Masignani, V., Eickmann, M., Becker, S., Abrignani, S., Klenk, H.-D., Rappuoli, R., 2003. SARS – beginning to understand a new virus. Nat. Rev. Microbiol. 1, 209–218, http://dx.doi.org/10.1038/nrmicro775.
Subissi, L., Imbert, I., Ferron, F., Collet, A., Coutard, B., Decroly, E., Canard, B., 2014a. SARS-CoV ORF1b-encoded nonstructural proteins 12–16: replicative enzymes as antiviral targets. Antiviral Res. 101, 122–130, http://dx.doi.org/10.1016/j.antiviral.2013.11.006.
Subissi, L., Posthuma, C.C., Collet, A., Zevenhoven-Dobbe, J.C., Gorbalenya, A.E., Decroly, E., Snijder, E.J., Canard, B., Imbert, I., 2014b. One severe acute respiratory syndrome coronavirus protein complex integrates processive RNA polymerase and exonuclease activities. Proc. Natl. Acad. Sci. U. S. A. 111, E3900–E3909, http://dx.doi.org/10.1073/pnas.1323705111.
Su, D., Lou, Z., Sun, F., Zhai, Y., Yang, H., Zhang, R., Joachimiak, A., Zhang, X.C., Bartlam, M., Rao, Z., 2006. Dodecamer structure of severe acute respiratory syndrome coronavirus nonstructural protein nsp10. J. Virol. 80, 7902–7908, http://dx.doi.org/10.1128/JVI.00483-06.
Sun, Y., Wang, Z., Tao, J., Wang, Y., Wu, A., Yang, Z., Wang, K., Shi, L., Chen, Y., Guo, D., 2014. Yeast-based assays for the high-throughput screening of inhibitors of coronavirus RNA cap guanine-N7-methyltransferase. Antiviral Res. 104, 156–164, http://dx.doi.org/10.1016/j.antiviral.2014.02.002.
Sutton, G., Fry, E., Carter, L., Sainsbury, S., Walter, T., Nettleship, J., Berrow, N., Owens, R., Gilbert, R., Davidson, A., Siddell, S., Poon, L.L.M., Diprose, J., Alderton, D., Walsh, M., Grimes, J.M., Stuart, D.I., 2004. The nsp9 replicase protein of SARS-coronavirus, structure and functional insights. Struct. Lond. Engl. 1993 (12), 341–353, http://dx.doi.org/10.1016/j.str.2004.01.016.
Tanner, J.A., Watt, R.M., Chai, Y.-B., Lu, L.-Y., Lin, M.C., Peiris, J.S.M., Poon, L.L.M., Kung, H.-F., Huang, J.-D., 2003. The severe acute respiratory syndrome (SARS) coronavirus NTPase/helicase belongs to a distinct class of 5′ to 3′ viral helicases. J. Biol. Chem. 278, 39578–39582, http://dx.doi.org/10.1074/jbc.C300328200.
Te Velthuis, A.J., Arnold, J.J., Cameron, C.E., van den Worm, S.H.E., Snijder, E.J., 2010. The RNA polymerase activity of SARS-coronavirus nsp12 is primer dependent. Nucleic Acids Res. 38, 203–214, http://dx.doi.org/10.1093/nar/gkp904.
Te Velthuis, A.J.W., van den Worm, S.H.E., Snijder, E.J., 2012. The SARS-coronavirus nsp7+nsp8 complex is a unique multimeric RNA polymerase capable of both de novo initiation and primer extension. Nucleic Acids Res. 40, 1737–1747, http://dx.doi.org/10.1093/nar/gkr893.
Van Vliet, A.L.W., Smits, S.L., Rottier, P.J.M., de Groot, R.J., 2002. Discontinuous and non-discontinuous subgenomic RNA transcription in a nidovirus. EMBO J. 21, 6571–6580.
Vasiljeva, L., Merits, A., Auvinen, P., Kääriäinen, L., 2000. Identification of a novel function of the alphavirus capping apparatus. RNA 5′-triphosphatase activity of Nsp2. J. Biol. Chem. 275, 17281–17287, http://dx.doi.org/10.1074/jbc.M910340199.
Von Grotthuss, M., Wyrwicz, L.S., Rychlewski, L., 2003. mRNA cap-1 methyltransferase in the SARS genome. Cell 113, 701–702.
Wang, L.F., Eaton, B.T., 2007. Bats, civets and the emergence of SARS. Curr. Top. Microbiol. Immunol. 315, 325–344.
Wengler, G., Wengler, G., 1993. The NS 3 nonstructural protein of flaviviruses contains an RNA triphosphatase activity. Virology 197, 265–273, http://dx.doi.org/10.1006/viro.1993.1587.
Xiao, Y., Ma, Q., Restle, T., Shang, W., Svergun, D.I., Ponnusamy, R., Sczakiel, G., Hilgenfeld, R., 2012. Nonstructural proteins 7 and 8 of feline coronavirus form a 2:1 heterotrimer that exhibits primer-independent RNA polymerase activity. J. Virol. 86, 4444–4454, http://dx.doi.org/10.1128/JVI.06635-11.
Zaki, A.M., van Boheemen, S., Bestebroer, T.M., Osterhaus, A.D.M.E., Fouchier, R.A.M., 2012. Isolation of a novel coronavirus from a man with pneumonia in Saudi Arabia. N. Engl. J. Med. 367, 1814–1820, http://dx.doi.org/10.1056/NEJMoa1211721.
Zhai, Y., Sun, F., Li, X., Pang, H., Xu, X., Bartlam, M., Rao, Z., 2005. Insights into SARS-CoV transcription and replication from the structure of the nsp7-nsp8 hexadecamer. Nat. Struct. Mol. Biol. 12, 980–986, http://dx.doi.org/10.1038/nsmb999.
Zirkel, F., Kurth, A., Quan, P.-L., Briese, T., Ellerbrok, H., Pauli, G., Leendertz, F.H., Lipkin, W.I., Ziebuhr, J., Drosten, C., Junglen, S., 2011. An insect nidovirus emerging from a primary tropical rainforest. mBio 2, e00011–e00077, http://dx.doi.org/10.1128/mBio.00077-11.
Zuo, Y., Deutscher, M.P., 2001. Exoribonuclease superfamilies: structural analysis and phylogenetic distribution. Nucleic Acids Res. 29, 1017–1026.
Züst, R., Cervantes-Barragan, L., Habjan, M., Maier, R., Neuman, B.W., Ziebuhr, J., Szretter, K.J., Baker, S.C., Barchet, W., Diamond, M.S., Siddell, S.G., Ludewig, B., Thiel, V., 2011. Ribose 2′-O-methylation provides a molecular signature for the distinction of self and non-self mRNA dependent on the RNA sensor Mda5. Nat. Immunol. 12, 137–143, http://dx.doi.org/10.1038/ni.1979.